**Proceedings of the 18th International Symposium on the Packaging and Transportation of Radioactive Materials
PATRAM 2016
September 18-23, 2016, Kobe, Japan**

Paper No. 2033

Impact analysis of the package having additional protector of orifice near the containment boundary of the primary lid in the drop test II

Minoru Nagai **Toshiya Kitamura**

Regulatory Standard and Research Department, Secretariat of Nuclear Regulation Authority (S/NRA/R)

Abstract

It is common to determine the suitability of drop test II as defined by the IAEA Specific Safety Requirements No.SSR-6 paragraph 727 for the condition in which the center of a vessel body or lid impacts a mild steel bar as it is considered to cause maximum damage. However, in case the package has an orifice protector (hereafter referred to as "protector") on the orifice cover, which constitutes a containment boundary, it is possible that the orifice cover will sustain damage. When a mild steel bar impacts the vicinity of the orifice, the protector could separate causing the mild steel bar to directly impact the orifice cover.

The behavior of the package when it impacts the mild steel bar through the protector was investigated. Case studies were conducted with finite element analyses (FEA) of a detailed model of the vicinity of the primarily lid and the protector. The parameters of the case study were the impact angles, impact points, and weld joint efficiencies between the protector and the cover plate of the shock absorber.

The FEA indicated that for some values of weld joint efficiency, the protector got separated owing to a rupture of the welding joint and the orifice cover protecting the orifice was directly impacted by the mild steel bar, producing a large amount of stress in the orifice cover. Damage to the orifice cover is a concern.

It was therefore concluded that it is necessary to consider an impact between the protector and the mild steel bar in drop test II for a package that has the protector on the primary lid.

Introduction

IAEA Specific Safety Requirements No.SSR-6 paragraph 727[1] requires that a package shall be dropped to experience maximum damage in the drop test. A test in which the package is dropped from a height of 1 m onto a mild steel bar is defined as drop test II in the requirements. It is common to determine the suitability of drop test II in the condition where the center of a vessel body or lid impacts a mild steel bar as it is considered to cause the maximum damage. For a package with a flat lid surface, the determination conforms to the requirement.

However, in the case of a package having a protector on the orifice cover, which constitutes a containment boundary, it is possible that there is damage to the orifice cover. When a mild steel bar impacts the vicinity of the orifice, the protector separates from the primary lid and the orifice cover directly impacts the mild steel bar. Therefore, the behavior of the package when it impacts the mild steel bar was investigated through several analyses.

Finite Element Analysis of package with additional protector

FEA of drop test II was conducted using the SIMULIA ABAQUS 6.14/Explicit. A schematic diagram of the drop test II model is shown in Figure 1. The following were modeled using the software: a lid in the vicinity of the package namely the protector, the orifice cover, the cover plate of the shock absorber, and the primary lid.

Analysis Model

A schematic of the finite element model is shown in Figure 2. The model of the primary lid has a stepped column shape that was designed referring to a typical package. The diameter of the lid was approximately 2000 mm. The model of the primary lid had a built-in orifice and orifice cover. The model of the orifice cover had a circular plate shape. The cover plate of the shock absorber and the primary lid were fixed on their peripheries. The protector and the cover plate of the shock absorber were joined by batting weld and fillet weld, and the protector was located above the orifice cover. The model of the mild steel bar was a column having a diameter of 150 mm, a flat top surface, and an edge radius of 6 mm.

The model of the primary lid had the initial velocity equivalent to a 1 m drop. A package mass of approximately 120 ton was loaded at the center of gravity of the primary lid. In consideration of structural symmetry, the finite element model was a half model. The symmetric surface of the finite element model was applied a symmetrical boundary and the bottom face of the mild steel bar was applied to a fixed boundary. Linear eight-node brick reduced integration elements were used. The number of elements was approximately 30,000.

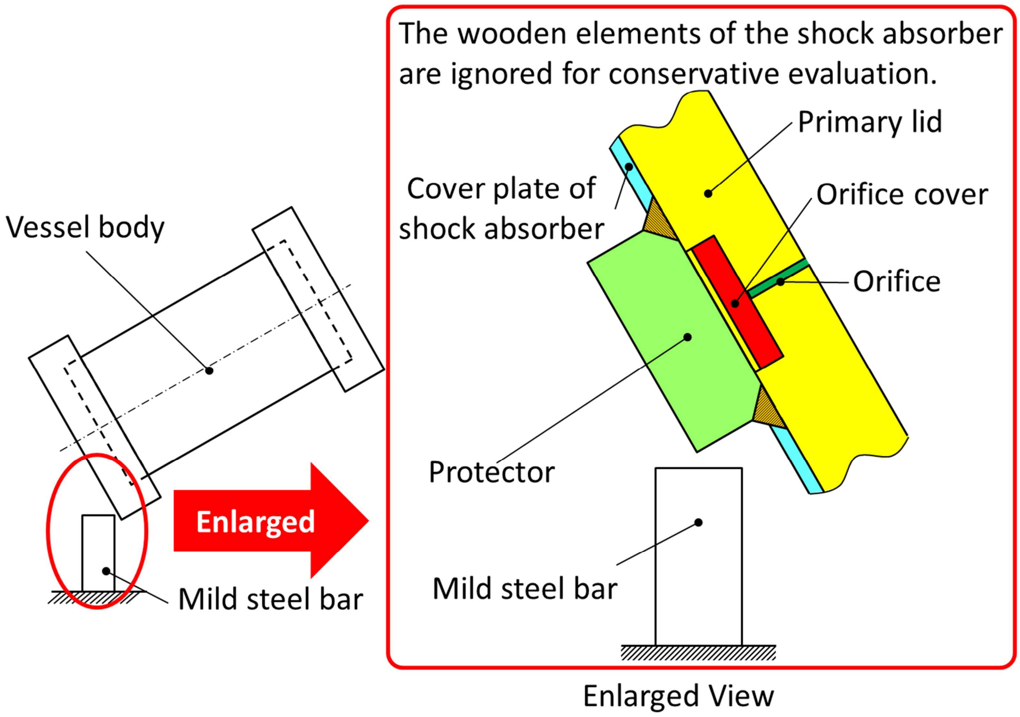

Figure 1. Schematic diagram of drop test model

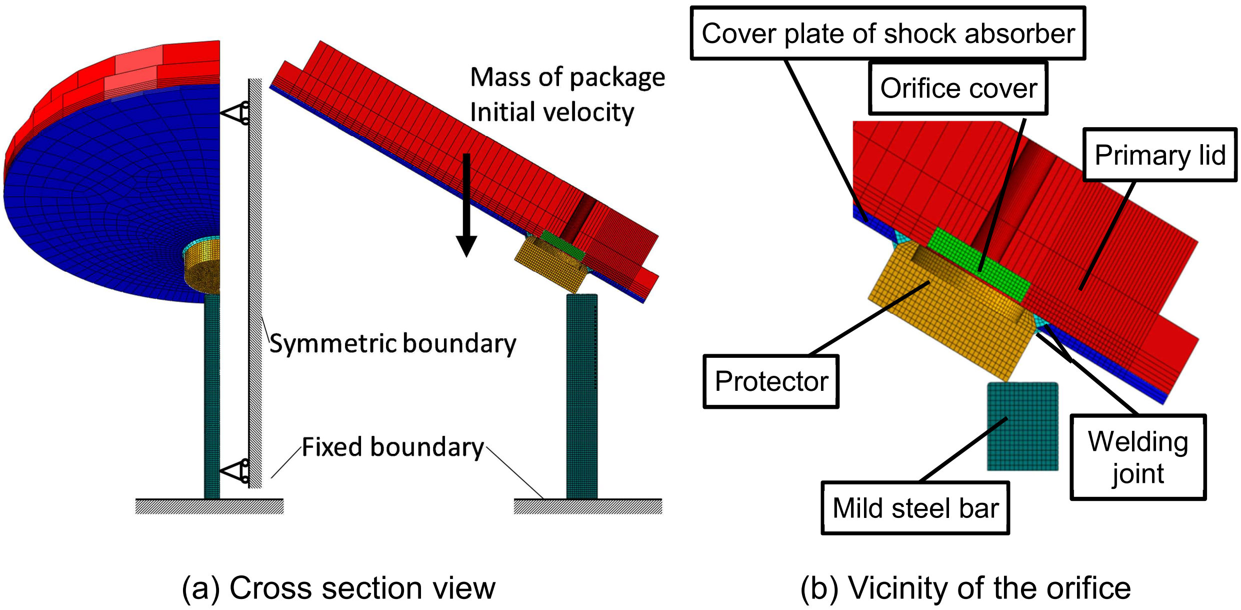

Figure 2. Finite element model of package having protector

Materials

All parts of the package, namely the protector, the primary lid, the cover plate of the shock absorber, and the orifice cover, were made of AISI 304 stainless steel. The mild steel bar was made of ASTM A36 mild steel.

The material properties of AISI 304 stainless steel and ASTEM A36 mild steel were applied using well known Johnson and Cook's plasticity and Johnson and Cook's dynamic ductile failure model. Johnson and Cook's plasticity is suitable for describing the plastic deformation on the large strain and high strain rate.

Johnson and Cook's plasticity constitutive equation can be expressed as follows:

$$\sigma_{eq} = \left(A + B\varepsilon_{eq}^{n}\right)\left(1 + C\ln\dot{\varepsilon}_{eq}^{*}\right)\left(1 - T^{*m}\right), \tag{1}$$

where σ_{eq} is the equivalent stress, ε_{eq} is the equivalent plastic strain, $\dot{\varepsilon}^{*}{}_{eq}$ is the reference strain rate, A, B, C, n, and m are material parameters, and T^{*} is the non-dimensional temperature. The parameters of Johnson and Cook's plasticity equation were decided based on the references [2, 3].

Johnson and Cook's dynamic failure equation can be expressed as follows:

$$\varepsilon_{D} = \left[d_1 + d_2 \exp\left(-d_3\eta\right)\right]\left[1 + d_4 \ln\left(\frac{\dot{\varepsilon}_{eq}^{*}}{\dot{\varepsilon}_{eq}}\right)\right]\left(1 + d_5 T^{*}\right), \tag{2}$$

where $d_1 \sim d_5$ are the failure parameters, η is the stress triaxiality, $\dot{\varepsilon}_{eq}$ is the equivalent plastic strain rate, $\dot{\varepsilon}^{*}{}_{eq}$ is the reference strain rate, and T^{*} is the non-dimensional temperature. The parameters of Johnson and Cook's dynamic failure model were decided based on the references [2, 3].

Failure criteria of the welding joint can be described by the following formula:

$$\max\left\{\frac{\langle T\rangle}{T_o}, \frac{S}{S_o}\right\} = 1, \tag{3}$$

Where T is tensile stress, S is shear stress, and < > is the Macaulay bracket that means <x> = 0 (x<0) or x (x≥0). T_o and S_o are the criteria of tensile and shear stresses, which depend on weld joint efficiency.

Analysis Cases

Twenty-seven cases of parametric study (standard analysis) were made using three parameters—namely impact points, impact angles, and weld joint efficiencies. Each parameter has three values, as shown in Figure 3 and Table 1. In addition, 18 analyses (additional analyses) were conducted as shown in Figure 4, Table 2, and Table 3, for two parameters—namely, weld leg length and coefficients of friction between the mild steel bar and the protector or the orifice cover. Each parameter has a different value from those of the standard analysis.

Analyses were also conducted using a detailed orifice cover model in order to consider the influence of the shape of the orifice on impact behavior. In the detailed orifice cover analysis, bolt- holes, and a round key of the orifice cover, the test orifice, and its plug were all modeled as shown in Figure 5. These detailed structures were not modeled in the standard analysis and additional analysis. The orifice model of these analyses is referred to as the simplified orifice cover model. The analyses for the detailed cover model were conducted at impact point 2, impact angles of 45° and 60°, and 50 % weld joint efficiency, as shown in Table 4. The weld leg length and friction coefficient were the same as those of the standard analyses.

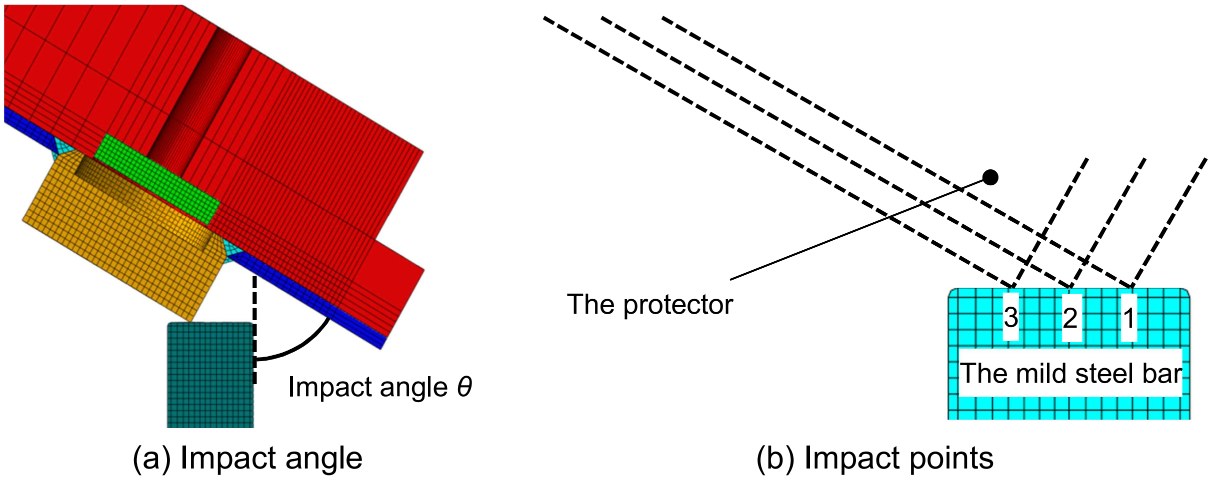

Figure 3. Parameters of finite element analysis

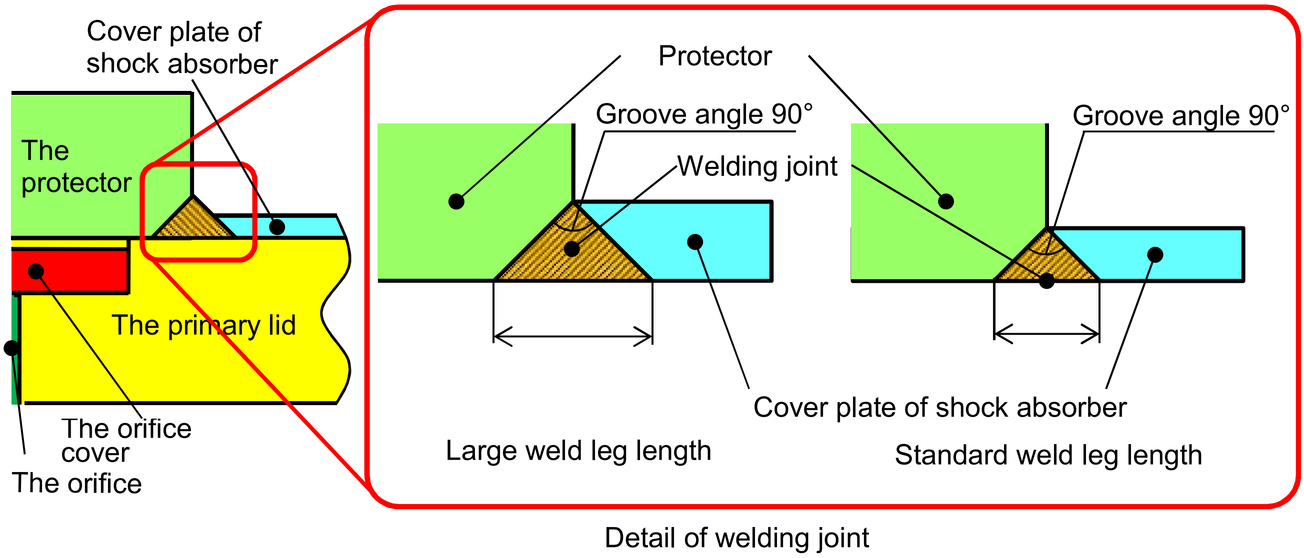

Figure 4. Large weld length model

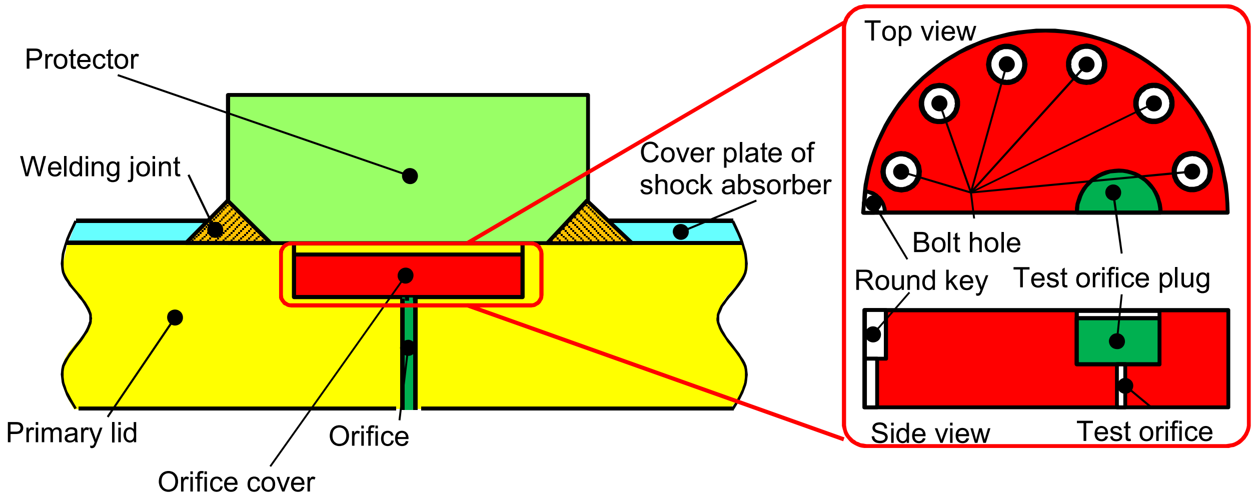

Figure 5. Detailed orifice cover model

Table 1. Parameters of standard analysis

Impact angle	Impact point	Weld joint efficiency	Coefficient of friction	Total case
30°, 45°, 60°	3 points	50 %, 70 %, 90 %	0.1	27

Table 2. Parameters of additional analysis in respect to weld leg length (in simplified orifice cover model)

Impact angle	Impact point	Weld joint efficiency	Weld leg length	Total case
30°, 45°, 60°	3 points	50 %, 90 %	(standard), large	18

Table 3. Parameters of additional analysis in respect to coefficient of friction (in simplified orifice cover model)

Impact angle	Impact point	Weld joint efficiency	Coefficient of friction	Total case
30°, 45°, 60°	3 points	50 %, 90 %	(0.1), 0.25	18

Table 4. Parameters of analysis in respect to detailed orifice cover model

Impact angle	Impact point	Weld joint efficiency	Coefficient of friction	Total case
45°, 60°	1 point (Impact point 2)	50 %	0.1	2

Analysis Results

Results of the standard analysis with respect to the impact points are shown in Figure 6. Figures 6 (a), (b), and (c) show the result of impact point 1, 3, and 2 respectively. These results were classified into the following three patterns of after-impact behavior of the protector and the mild steel bar.

Pattern A: The protector did not separate from the primary lid.

Pattern B: The protector separated from the surface of the primary lid but the orifice cover did not impact the mild steel bar.

Pattern C: The protector separated from the surface of the primary lid and the orifice cover impacted the mild steel bar.

Figure 6 (a), (b), and (c) are Pattern A, Pattern B, and Pattern C respectively. The results of the standard analysis were classified into these three patterns and were shown in Table 5.

Figure 7 shows the results of the standard analysis with respect to impact angle. In the case of θ = 30° shown in Figure 7 (a), the protector did not separate (Pattern A). In the case of θ = 45° and 60° shown in Figures 7 (b) and (c), the protector separated and the orifice cover impacted the mild steel bar (Pattern C).

Figure 8 shows the results of the standard analysis with respect to weld joint efficiency. In the case of 50 % and 70 % weld joint efficiency shown in Figures 8 (a) and (b), the protector separated and the orifice cover impacted the mild steel bar (Pattern C). In the case of 90 % weld joint efficiency shown in Figure 8 (c), the protector did not separate (Pattern A).

The results of additional analysis were classified and shown in Table 6 and Table 7. The results of these analyses show a tendency similar to that of the standard analysis, while several results, which are surrounded by red circles on the Table 6 and Table 7, were different.

Figure 9 (a) and (b) show the equivalent stress of the orifice cover by using the simplified orifice cover model. Figures 9 (c) and (d) show the equivalent stress in the detailed orifice cover model. The maximum stresses of the simplified orifice cover models were 420 MPa in the case of a 45° impact angle and 450 MPa in the case of a 60° impact angle. The maximum stresses of the detailed orifice cover model were 500 MPa in the case of a 45° impact angle and 690 MPa in the case of 60° impact angle.

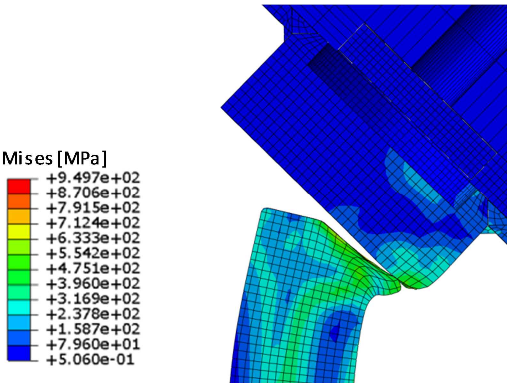

(a) Pattern A (impact point 1)

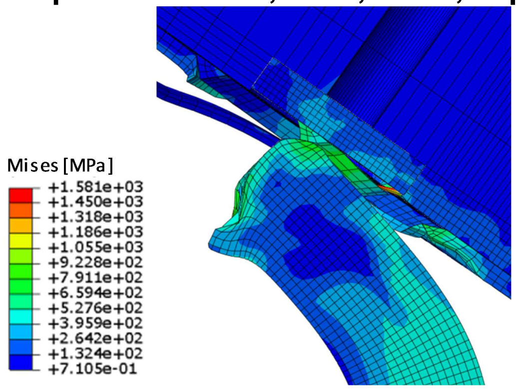

(b) Pattern B (impact point 3)

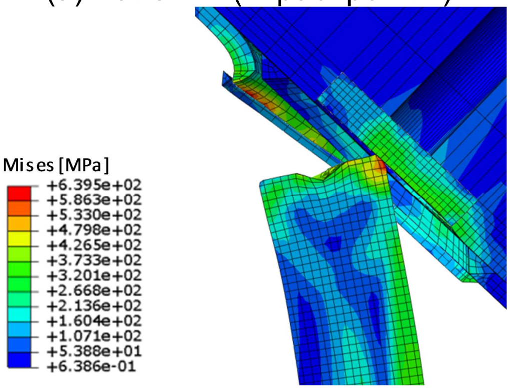

(c) Pattern C (impact point 2)

Constant parameters: θ = 45°, weld joint efficiency 70 %

Figure 6. Results of standard analysis in respect to impact point

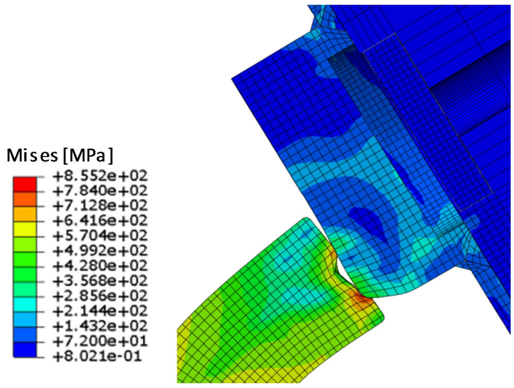

a) 30°

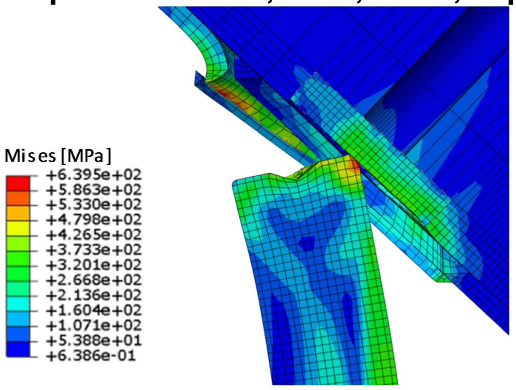

(b) 45°

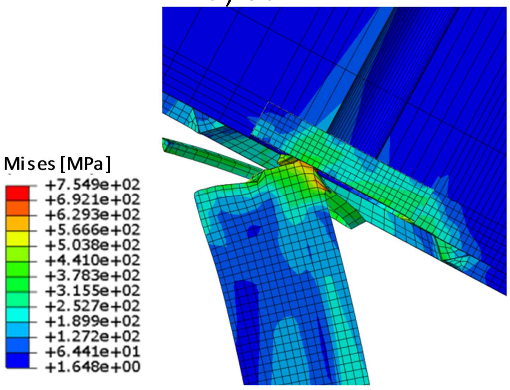

(c) 60°

Constant parameters: Impact point 2, weld joint efficiency 70 %

Figure 7. Results of standard analysis in respect to impact angle

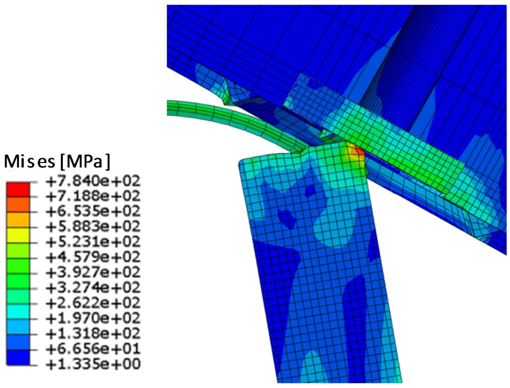

(a) 50 %

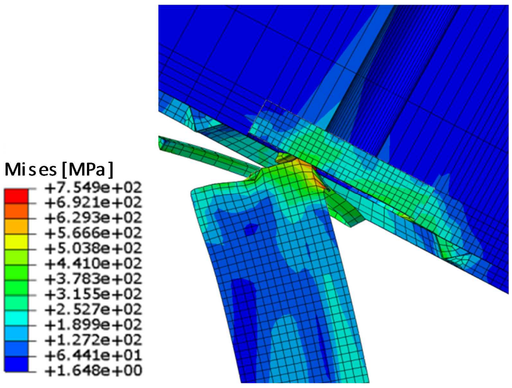

(b) 70 %

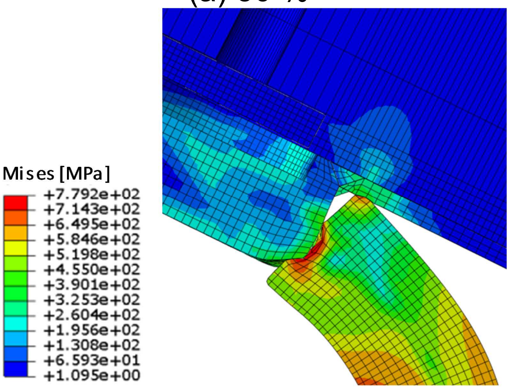

(c) 90 %

Constant parameters: Impact point 2, θ = 60°

Figure 8. Results of standard analysis with respect to weld joint efficiency

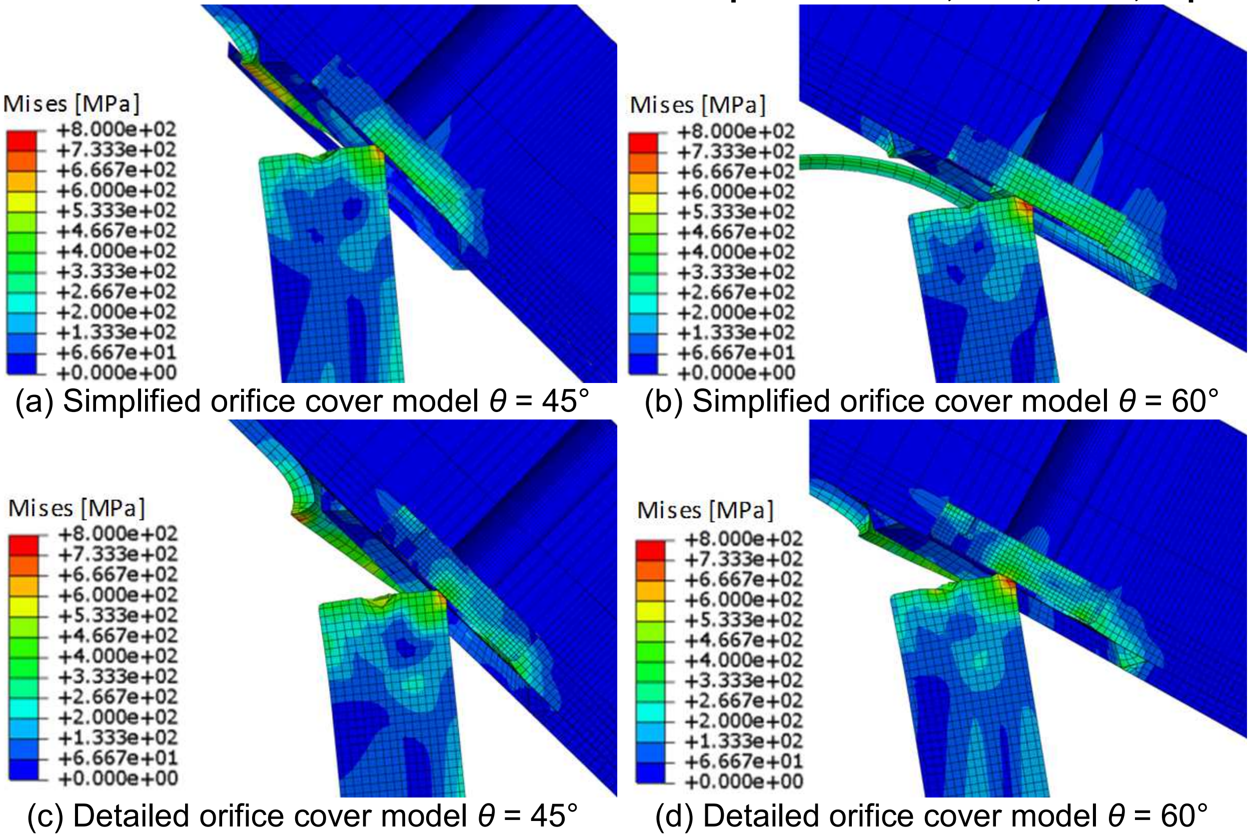

Figure 9. Stress distribution of orifice cover (Simplified and Detailed orifice cover model)

Table 5. Results of standard analysis

Impact angle		**30°**			**45°**			**60°**		
Weld joint efficiency		50 %	70 %	90 %	50 %	70 %	90 %	50 %	70 %	90 %
Impact point	**1 (right side)**	A	A	A	A	A	A	C	A	A
	2 (center)	B	A	A	C	C	A	C	C	A
	3 (left side)	B	B	B	C	B	A	C	A	A

A: The protector did not separate
B: The protector separated from the surface of the primary lid and the orifice cover did not impact onto the mild steel bar.
C: The protector separated from the surface of the primary lid and the orifice cover impacted onto the mild steel bar.

Table 6. Analysis results of large coefficient of the friction

Impact angle		**30°**		**45°**		**60°**	
Weld joint efficiency		50 %	90 %	50 %	90 %	50 %	90 %
Impact point	**1 (right side)**	A	A	A	A	B	A
	2 (center)	B	A	C	A	C	A
	3 (left side)	B	B	C	A	A	A

Table 7. Analysis results of large weld leg length

Impact angle		30°		45°		60°	
Weld joint efficiency		50 %	90 %	50 %	90 %	50 %	90 %
Impact point	1 (right side)	A	A	A	A	C	A
	2 (center)	A	A	C	A	C	A
	3 (left side)	B	B	B	A	C	A

Discussion

Table 5 shows that the cases where the protector was prone to separating from the primary lid (Pattern B or pattern C) are shown as follows.

- Low weld joint efficiency
- Impact point 2 or 3

The shift of impact point made the difference in the behavior of the mild steel bar. For example in the case of impact point 3, the bending direction of the mild steel bar was different from that of the other impact points. It is considered that the difference in behavior of the mild steel bar causes a difference in the impact behavior.

The cases where the orifice cover was prone to impact with the mild steel bar (Pattern C) are shown below.

- 45°or 60° impact angle

Comparing Tables 5, 6, and 7, there was little difference in the after-impact behavior of the standard analysis and the additional analysis. The result of the additional analysis indicated that large coefficient of friction or the large weld leg length case made it hard to separate the protector from the orifice.

The equivalent stresses on the orifice cover shown in Figure 9 were larger than the yield stress of AISI 304 stainless steel 205 MPa. This means that when the orifice cover impacts the mild steel bar, a yield (separation) of the top surface of the orifice cover could occur.

Conclusions

The conclusions from FEA of the package with an additional protector of the orifice are as follows.

- The analyses indicated that for some values of weld joint efficiency, the protector could separate from the primary lid owing to the impact with the steel bar.
- The analyses also indicated that the cover of the orifice could impact the mild steel bar

after the separation of the protector.

- The difference in the impact angle, impact point, and weld joint efficiency affected the possibility of the separation of the protector and the impact of the orifice cover onto the mild steel bar.
- The maximum equivalent stress of the cover of the orifice is greater than the yield stress of the AISI 304 stainless steel when the cover of the orifice impacts the mild steel bar.

In conclusion, it was preferable to take into account an impact between the protector and the mild steel bar in drop test II for packages that have a protector. The consideration of the impact angle, impact point, and weld joint efficiency was particularly important.

References

[1] International Atomic Energy Agency (IAEA), Regulations for the Safe Transport of Radioactive Material, 2012 Edition, Specific Safety Requirements No. SSR-6, 2012.
[2] Jaime Fronta´n et al., Ballistic performance of nanocrystalline and nanotwinned ultrafine crystal steel, Acta MATERIALIA, 2012.
[3] Jeremy D. Seidt et al., High Strain Rate, High Temperature Constitutive and Failure Models for EOD Impact Scenarios, Proceedings of the 2007 SEM Annual Conference and Exposition on Experimental and Applied Mechanics, Springfield, 2007.